Influences of Ligand Environment on the Spectroscopic Properties and Disproportionation Reactivity of Copper−Nitrosyl Complexes

Jamie L. Schneider, Susan M. Carrier, Christy E. Ruggiero, Victor G. Young, Jr., and William B. Tolman*

Contribution from the Department of Chemistry and Center for Metals in Biocatalysis, University of Minnesota, 207 Pleasant Street S.E., Minneapolis, Minnesota 55455

Received June 22, 1998

Abstract: In studies of the chemistry of new copper−nitrosyl complexes supported by tris(3-(trifluoromethyl)-5-methylpyrazol-1-yl)hydroborate (Tp^{CF_3,CH_3}) and tris(3-mesitylpyrazol-1-yl)hydroborate ($Tp^{Ms,H}$), significant effects of the scorpionate ligand substituents on the properties of the $\{CuNO\}^{11}$ unit were found that have implications for environmental influences on similar species in biological and catalytic systems. The copper(I) complexes $Tp^{Ms,H}Cu(THF)$ and $Tp^{CF_3,CH_3}Cu(CH_3CN)$ were structurally characterized by X-ray crystallography, and their respective CO and NO adducts were studied by FTIR, EPR, NMR, and/or UV−vis spectroscopies in solution. Both nitrosyl complexes disproportionate in the presence of excess NO to N_2O and $Tp^{R,R'}Cu(NO_2)$; an X-ray structure of the latter product supported by Tp^{CF_3,CH_3} was determined. Unlike previously studied paramagnetic $[CuNO]^{11}$ compounds that exhibit EPR signals with $g < 2.0$ and large A^{NO} values at temperatures below ~40 K (Ruggiero, C. E.; Carrier, S. M.; Antholine, W. E.; Whittaker, J. W.; Cramer, C. J.; Tolman, W. B. *J. Am. Chem. Soc.* **1993**, *115*, 11285−11298), $Tp^{Ms,H}Cu(NO)$ is EPR silent at 4.2 K and exhibits an NMR spectrum (238 K, toluene-d_8) with sharp signals. Peak assignments for the NMR spectrum were deduced from integrated intensities, temperature-dependent isotropic shifts, and the nuclear relaxation rates. The unique NMR spectral behavior for the $Tp^{Ms,H}$ complex, which only differs from those of analogues with simple phenyl substituents by virtue of the shape of the substrate binding pocket enforced by the mesityl methyl groups, suggests that caution should be exercised in characterizing such adducts in proteins and heterogeneous systems; subtle environmental effects may determine the applicability of EPR versus NMR methods. The electron-withdrawing effects of the trifluoromethyl substituents in $Tp^{CF_3,CH_3}Cu(NO)$ perturb $\nu(NO)$ and the Cu(I) → NO MLCT energy in the respective FTIR and UV−vis spectra and induce a significant slowing of its disproportionation rate. These results, in conjunction with those obtained from kinetic and spectroscopic studies on the $Tp^{Ms,H}$ system, support a mechanism for the disproportionation involving generation of the CuNO adduct from NO and the Cu(I) precursor in a preequilibrium step, followed by electrophilic attack of a second NO molecule on the adduct that is rate-controlling.

Introduction

Copper−nitrosyl (CuNO) adducts are implicated in the reactions of metalloproteins with bioactive nitric oxide and are pivotal intermediates in biological and catalytic systems that participate in environmentally significant nitrogen oxide processing. Thus, in bacterial denitrification, a key component of the global nitrogen cycle whereby NO_3^- and NO_2^- are reduced to gaseous N_2O and/or N_2, a $[CuNO]^{2+}$ species is a purported intermediate during copper nitrite reductase turnover.[1] Numerous other copper proteins have been probed by purposeful addition of NO (e.g., as an O_2 surrogate), and some of the varied effects of biosynthesized[2] NO may arise from these or related Cu−NO adducts.[3] For example, the cytotoxicity of NO may be traced in part to its inhibition of mitochondrial cytochrome *c* oxidase, for which both copper and heme-iron adducts have been identified.[3c,d] In addition to these biological cases, Cu zeolites have been found to be highly active for the catalytic decomposition of NO.[4] The many potential applications of these materials in heterogeneous NO_x removal from gas streams has motivated several studies of (zeolite)Cu−NO intermediates by both experimental and theoretical methods.[4,5]

In efforts to understand the fundamental chemistry of CuNO species in detail and, ultimately, to control the reactivity of this interesting unit, we[6] and others[7] have targeted discrete copper−nitrosyl complexes for synthesis and physicochemical characterization.[8] Previously, we reported the only X-ray crystal structure of a mononuclear complex, $Tp^{tBu,H}Cu(NO)$ (Figure 1),[9] and defined its electronic structure through spectroscopic and

* To whom correspondence should be addressed. Fax: 612-624-7029. E-mail: tolman@chem.umn.edu.

(1) Averill, B. A. *Chem. Rev.* **1996**, *96*, 2951−2964.

(2) (a) Crane, B. R.; Arvai, A. S.; Ghosh, D. K.; Wu, C.; Getzoff, E. D.; Stuehr, D. J.; Tainer, J. A. *Science* **1998**, *279*, 2121−2126. (b) Crane, B. R.; Arvai, A. S.; Gachhui, R.; Wu, C.; Ghosh, D. K.; Getzoff, E. D.; Stuehr, D. J.; Tainer, J. A. *Science* **1997**, *278*, 425−431. (c) Marletta, M. A. *J. Biol. Chem.* **1993**, *268*, 12231−12234.

(3) Selected lead references: (a) Gorren, A. C. F.; de Boer, E.; Wever, R. *Biochim. Biophys. Acta* **1987**, *916*, 38−47. (b) Musci, G.; Marco, S. D.; di Patti, M. C. B.; Calabrese, L. *Biochemistry* **1991**, *30*, 9866−9872. (c) Zhao, X.-J.; Sampath, V.; Caughey, W. S. *Biochem. Biophys. Res. Commun.* **1994**, *204*, 537−543. (d) Cooper, C. E.; Torres, J.; Sharpe, M. A.; Wilson, M. T. *FEBS Lett.* **1997**, *414*, 281−284. (e) Ehrenstein, D.; Filiaci, M.; Scharf, B.; Engelhard, M.; Steinbach, P. J.; Nienhaus, G. U. *Biochemistry* **1995**, *34*, 12170−12177.

(4) Shelef, M. *Chem. Rev.* **1995**, *95*, 209−225.

(5) Selected recent lead references: (a) Sojka, Z.; Che, M. *J. Phys. Chem. B* **1997**, *101*, 4831−4838. (b) Schneider, W. F.; Hass, K. C.; Ramprasad, R.; Adams, J. B. *J. Phys. Chem.* **1996**, *100*, 6032−6046. (c) Wichterlová, B.; Sobalík, Z.; Vondrová, A. *Catal. Today* **1996**, *29*, 149−153.

10.1021/ja982172q CCC: $15.00
Published on Web 10/21/1998

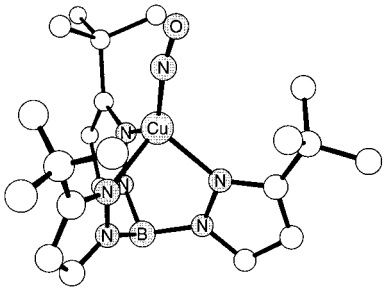

Figure 1. Chem3D representation of the X-ray crystal structure of $Tp^{tBu,H}CuNO$, with hydrogen atoms omitted for clarity.[6c]

ab initio theoretical studies.[6a,c] A molecular orbital description of the bonding of the {CuNO}[11] species was proposed in which the copper d orbital manifold is full and the SOMO extends over the entire unit but has a primary contribution from a NO π^* orbital [i.e., Cu(I)−NO$^\bullet$ with significant covalency].[6c,10] Consistent with this picture, the complex exhibits an EPR signal at temperatures below ∼40 K with $g_e \sim g_\perp > g_\parallel = 1.83$, $A_\perp^{Cu} = 62 \times 10^{-4}$ cm^{-1}, and $A^{NO} = 27 \times 10^{-4}$ cm^{-1}, no absorption or MCD intensity in the metal d → d transition region, and a Cu → NO MLCT band with $\lambda_{max} = 494$ nm ($\epsilon \sim 1400$ M^{-1} cm^{-1}). Analogous compounds with similar spectroscopic properties were prepared using ligands with phenyl ($Tp^{Ph,Ph}$) or methyl (Tp^{CH_3,CH_3}) substituents, but the decreased steric hindrance in these instances relative to $Tp^{tBu,H}$ rendered the complexes unstable with respect to disproportionation (eq 1).[6d]

$$Tp^{R,R'}Cu(NO) + 2NO \rightarrow Tp^{R,R'}Cu(NO_2) + N_2O \quad (1)$$

Preliminary kinetics and isotope labeling studies confirmed the reaction stoichiometry and showed that the decay rate dependence on [TpCu(NO)] was first-order, thus ruling out a rate-determining dimerization but providing little information on the order with respect to NO and the nature of the critical N−N bond formation step.

In view of the various different environments (multiple proteins, zeolites) within which Cu−NO adducts may reside and the possible repercussions of such differences on spectral properties and reactivity, we sought to examine more closely the consequences of changing the nature of the pocket surrounding the CuNO unit in the $Tp^{R,R'}$ complexes. Herein we report the results of studies of NO binding to new Cu(I) complexes supported by the known scorpionates Tp^{CF_3,CH_3} [11] and $Tp^{Ms,H}$.[12] The former ligand is only marginally more sterically hindered than Tp^{CH_3,CH_3} but, due to the fluorine substitution, is significantly more electron withdrawing. The ortho methyl groups on the phenyl rings of $Tp^{Ms,H}$ restrict rotation of the mesityl substituents and induce adoption of an active-site pocket comprising a "wall" of aromatic groups approximately orthogonal to the pyrazolyl rings. We have found that both perturbations, the electron withdrawal by Tp^{CF_3,CH_3} and the particular pocket geometry induced by $Tp^{Ms,H}$, impact the chemistry of the CuNO unit significantly. The observed influences of the ligand substituents on the spectroscopic features and/or reactivity of the copper nitrosyls imply that environmental effects on such species in proteins and heterogeneous systems may be severe.

Results

Copper(I) Complexes. The starting materials $Tp^{Ms,H}$-Cu(THF) and $Tp^{CF_3,CH_3}Cu(CH_3CN)$ were isolated as colorless crystalline solids in moderate yields by respective treatment in THF of $TlTp^{Ms,H}$ with CuCl and of $NaTp^{CF_3,CH_3}$ with $[Cu(CH_3CN)_4]SbF_6$. Isolation of the $Tp^{Ms,H}$ complex as a monomer under these reaction conditions was surprising, both because structurally defined Cu(I)−THF adducts are rare[13] and because analogous preparations with other $Tp^{R,R'}$ ligands (R = R′ = H, CH_3, or Ph; R = tBu, R′ = H or CH_3) yield dimeric complexes of formula $[Tp^{R,R'}Cu]_2$.[14] The THF molecule may be removed either by recrystallizing the complex in the absence of free THF or by exposing the solid to a vacuum. The resulting species analyzes correctly for $[Tp^{Ms,H}Cu]_x$, but its exact nature is not known.

The structures of $Tp^{Ms,H}Cu(THF)$ and $Tp^{CF_3,CH_3}Cu(CH_3CN)$ were confirmed by X-ray crystallography; drawings are shown in Figures 2 and 3, crystallographic data are presented in Table 1, and selected interatomic distances and angles are listed in Table 2. Like other monomeric Cu(I) complexes of $Tp^{R,R'}$ ligands,[15] $Tp^{Ms,H}$ and Tp^{CF_3,CH_3} bind in tridentate fashion to the metal ion which has an additional fourth donor, THF and CH_3CN, respectively. In $Tp^{Ms,H}Cu(THF)$ (Figure 2), there is a crystallographic 3-fold axis passing through Cu(1) and B(1),

(6) (a) Carrier, S. M.; Ruggiero, C. E.; Tolman, W. B.; Jameson, G. B. *J. Am. Chem. Soc.* **1992**, *114*, 4407−4408. (b) Tolman, W. B.; Carrier, S. M.; Ruggiero, C. E.; Antholine, W. E.; Whittaker, J. W. In *Bioinorganic Chemistry of Copper*; Karlin, K. D., Tyeklár, Z., Eds.; Chapman & Hall, Inc.: New York, 1993; pp 406−418. (c) Ruggiero, C. E.; Carrier, S. M.; Antholine, W. E.; Whittaker, J. W.; Cramer, C. J.; Tolman, W. B. *J. Am. Chem. Soc.* **1993**, *115*, 11285−11298. (d) Ruggiero, C. E.; Carrier, S. M.; Tolman, W. B. *Angew. Chem., Int. Ed. Engl.* **1993**, *33*, 895−897. (e) Tolman, W. B. In *Mechanistic Bioinorganic Chemistry*; Thorp, H. H., Pecoraro, V. L., Eds.; ACS Symposium Series 246, American Chemical Society: Washington, DC, 1995; pp 195−217.

(7) (a) Paul, P. P.; Tyeklár, Z.; Farooq, A.; Karlin, K. D.; Liu, S.; Zubieta, J. *J. Am. Chem. Soc.* **1990**, *112*, 2430−2432. (b) Paul, P. P.; Karlin, K. D. *J. Am. Chem. Soc.* **1991**, *113*, 6331−6332. (c) Mercer, M.; Fraser, R. T. M. *J. Inorg. Nucl. Chem.* **1963**, *25*, 525−534. (d) Fraser, R. T. M. *J. Inorg. Nucl. Chem.* **1961**, *17*, 265−272. (e) Doyle, M. P.; Siegfried, B.; Hammond, J. J. *J. Am. Chem. Soc.* **1976**, *98*, 1627−1629.

(8) Examples of reactions of NO with copper complexes wherein formation of an adduct is implicated but is not amenable to direct characterization: (a) Tran, D.; Ford, P. C. *Inorg. Chem.* **1996**, *35*, 2411−2412. (b) Deters, D.; Weser, U. *BioMetals* **1995**, *8*, 25−29. (c) Tran, D.; Skelton, B. W.; White, A. H.; Laverman, L. E.; Ford, P. C. *Inorg. Chem.* **1998**, *37*, 2505−2511.

(9) (a) Abbreviations used (according to ref 9b): $Tp^{tBu,H}$ = tris(3-*tert*-butylpyrazol-1-yl)hydroborate; Tp^{CH_3,CH_3} = tris(3,5-dimethylpyrazol-1-yl)-hydroborate; Tp^{CF_3,CH_3} = tris(3-(trifluoromethyl)-5-methylpyrazol-1-yl)-hydroborate; $Tp^{Ms,H}$ = tris(3-mesitylpyrazol-1-yl)hydroborate; $Tp^{Ph,Ph}$ = tris(3,5-diphenylpyrazol-1-yl)hydroborate. (b) Trofimenko, S. *Chem. Rev.* **1993**, *93*, 943−980.

(10) Other theoretical calculations on bare {CuNO}[11] agree with this view: Thomas, J. L. C.; Bauschlicher, C. W., Jr.; Hall, M. B. *J. Phys. Chem. A* **1997**, *101*, 8530−8539 and references therein.

(11) (a) Bucher, U. E.; Currao, A.; Nesper, R.; Rüegger, H.; Venanzi, L. M.; Younger, E. *Inorg. Chem.* **1995**, *34*, 66−74. (b) Bucher, U. E. Ph.D. Thesis, Swiss Federal Institute of Technology, 1993.

(12) Rheingold, A. L.; White, C. B.; Trofimenko, S. *Inorg. Chem.* **1993**, *32*, 3471−3477.

(13) (a) Munakata, M.; Wu, L. P.; Kuroda-Sowa, T.; Maekawa, M.; Suenaga, Y.; Furuichi, K. *J. Am. Chem. Soc.* **1996**, *118*, 3305−3306. (b) El-Amouri, H.; Bahsoun, A. A.; Fischer, J.; Osborn, J. A.; Youinou, M.-T. *Organometallics* **1991**, *10*, 3582−3588. (c) Zakharov, L. N.; Saf'yanov, Y. N.; Struchkov, Y. T.; Abakumov, G. A.; Cherkasov, V. K.; Garnov, V. A. *Koord. Khim.* **1990**, *16*, 802.

(14) (a) Mealli, C.; Arcus, C. S.; Wilkinson, J. L.; Marks, T. J.; Ibers, J. A. *J. Am. Chem. Soc.* **1976**, *98*, 711−718. (b) Carrier, S. M.; Ruggiero, C. E.; Houser, R. P.; Tolman, W. B. *Inorg. Chem.* **1993**, *32*, 4889−4899. (c) Yoon, K.; Parkin, G. *Polyhedron* **1995**, *14*, 811−821. (d) Kiani, S.; Long, J. R.; Stavropoulos, P. *Inorg. Chim. Acta* **1997**, *263*, 357−366.

(15) (a) Kitajima, N.; Fujisawa, K.; Fujimoto, C.; Moro-oka, Y.; Hashimoto, S.; Kitagawa, T.; Toriumi, K.; Tatsumi, K.; Nakamura, A. *J. Am. Chem. Soc.* **1992**, *114*, 1277−1291. (b) Dias, H. V. R.; Lu, H.-L. *Inorg. Chem.* **1995**, *34*, 5380−5382. (c) Dias, H. V. R.; Kim, H.-J.; Lu, H.-L.; Rajeshwar, K.; de Tacconi, N. R.; Derecskei-Kovacs, A.; Marynick, D. S. *Organometallics* **1996**, *15*, 2994−3003. (d) Keyes, M. C.; Chamberlain, B. M.; Caltagirone, S. A.; Halfen, J. A.; Tolman, W. B. *Organometallics* **1998**, *17*, 1984−1992.

Table 1. X-ray Crystallographic Data

	$Tp^{Ms,H}Cu(THF)$	$Tp^{CF_3,CH_3}Cu(CH_3CN)$	$Tp^{CF_3,CH_3}Cu(NO_2)$
empirical formula	$C_{40}H_{48}BCuN_6O$	$C_{17}H_{16}BCuF_9N_7$	$C_{15}H_{13}BCuF_9N_7O_2$
formula weight	703.19	563.72	568.67
crystal system	trigonal	monoclinic	orthorhombic
space group	*R*3*c*	$P2_1/c$	Pnma
a (Å)	11.822(2)	11.936(2)	17.7811(5)
b (Å)	11.822(2)	8.954(2)	13.4460(4)
c (Å)	45.376(9)	21.890(4)	8.6908(2)
α (deg)	90	90	90
β (deg)	90	102.80 (3)	90
γ (deg)	120	90	90
V (Å^3)	5492(2)	2281.4(8)	2077.8(1)
Z	6	4	4
d(calcd), g cm^{-3}	1.276	1.641	1.818
temp (K)	173(2)	293(2)	173(2)
crystal size (mm)	0.60 × 0.50 × 0.30	0.50 × 0.50 × 0.50	0.22 × 0.22 × 0.03
diffractometer	Enraf-Nonius CAD4	Enraf-Nonius CAD4	Siemens SMART
abs coeff (mm^{-1})	0.637	1.051	1.161
θ range (deg)	2.18−25.99	2.29−25.04	2.29−25.06
hkl ranges	−14,−14,0 to 14,14,55	0,0,−25 to 14,10,25	0,0,0 to 21,16,10
no. of reflns collected	7289	4511	10311
no. of indep reflns	1225 (R_{int} = 0.065)	4008 (R_{int} = 0.1723)	1936 (R_{int} = 0.0342)
*R*1/w*R* ($I > 2\sigma(I)$)	0.0369/0.0891	0.0565/0.1474	0.0374/0.0771
*R*1/w*R*2 (all data)	0.0438/0.0929	0.1202/0.1890	0.0485/0.0810
goodness-of-fit (F^2)	1.062	1.010	1.093
largest diff features (e Å^{-3})	0.328 and −0.735	0.932 and −0.613	0.425 and −0.405

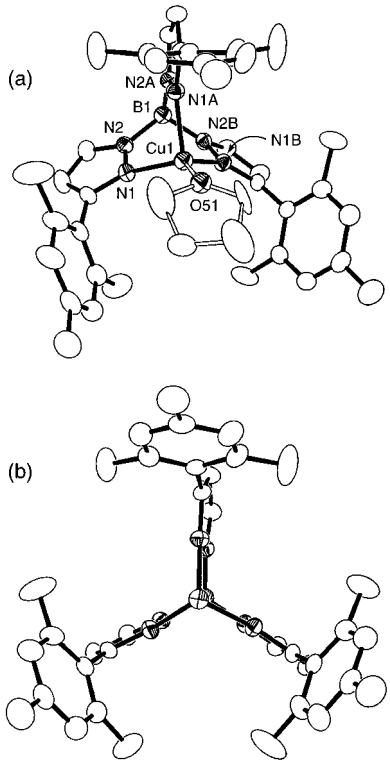

Figure 2. Representations of the X-ray crystal structure of $Tp^{Ms,H}$-Cu(THF) (50% ellipsoids; hydrogen atoms omitted for clarity); (a) full complex, heteroatoms labeled, with only one of three positions for the disordered THF molecule shown; (b) complex viewed along the Cu(1)−B(1) axis without the THF ligand.

but the THF molecule is displaced from this axis and thus is disordered over three positions. Because the THF oxygen atom O(51) resides only slightly off-axis, it displayed unreasonable anisotropic thermal parameters, so it was refined isotropically. Importantly, as in other structures with $Tp^{Ms,H}$,[12] and similar to the case of complexes of a related ligand with 9-anthryl substituents on the pyrazolyl groups (Tp^{Ant}),[16] the mesityl substituents lie orthogonal to their respective pyrazolyl rings to provide a substrate binding pocket in the fourth copper coordination position that is enclosed by three aromatic "walls" (Figure 2b). The complex $Tp^{CF_3,CH_3}Cu(CH_3CN)$ (Figure 3) lacks crystallographic 3-fold symmetry, has disordered CF_3 groups,

(16) Han, R.; Parkin, G. *Polyhedron* **1995**, *14*, 387−391.

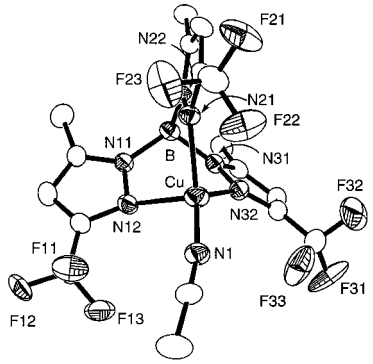

Figure 3. Representation of the X-ray crystal structure of Tp^{CF_3,CH_3}-Cu(CH_3CN) (30% ellipsoids; hydrogen atoms omitted for clarity; heteroatoms labeled).

Table 2. Selected Bond Lengths (Å) and Angles (deg)[a]

	$Tp^{Ms,H}Cu(THF)$		
Cu(1)−O(51)	2.004(7)	O(51)−Cu(1)-N(1)	129.6(4)
Cu(1)−N(1)	2.061(3)		
	$Tp^{CF_3,CH_3}Cu(CH_3CN)$		
Cu−N(1)	1.875(5)	Cu−N(22)	2.057(4)
Cu−N(32)	2.075(4)	Cu−N(12)	2.200(4)
N(1)−Cu−N(22)	134.8(2)	N(1)−Cu−N(32)	128.5(2)
N(22)−Cu(N(32)	90.0(2)	N(1)−Cu−N(12)	108.6(2)
N(22)−Cu−N(12)	92.8(2)	N(32)−Cu−N(12)	88.8(2)
	$Tp^{CF_3,CH_3}Cu(NO_2)$		
Cu(1)−N(2)	1.970(2)	Cu(1)−O(1)	2.003(2)
Cu(1)−N(4)	2.195(3)	Cu(1)−N(5)	2.439(4)
N(5)−O(1)	1.265(3)	N(2)−Cu(1)−N(2A)	89.77(13)
N(2)−Cu(1)−O(1A)	160.65(9)	N(2)−Cu(1)−O(1)	102.30(9)
O(1A)−Cu(1)−O(1)	62.33(13)	N(2)−Cu(1)−N(4)	90.79(9)
O(1)−Cu(1)−N(4)	103.93(10)	N(2)−Cu(1)−N(5)	132.58(7)
O(1)−N(5)−O(1A)	110.0(3)	N(4)−Cu(1)−N(5)	106.13(13)

[a] Estimated standard deviations indicated in parentheses.

Table 3. FTIR and UV−Vis Data for $Tp^{R,R'}Cu(L)$ (L = NO, CO)

ligand	ν(CO) (cm^{-1})	ν(^{14}NO) (cm^{-1})	ν(^{15}NO) (cm^{-1})	λ_{max} (nm) L = NO	ref
Tp^{CH_3,CH_3}	2060	*a*	*a*	494	6d, 14a
$Tp^{tBu,H}$	2069	1712	1679	494	6a,c
$Tp^{Ms,H}$	2079	1712	1682	472	this work
$Tp^{Ph,Ph}$	2086	1720	1687	474	15a, 6c
$Tp^{CF_3,H}$	2100				15b
Tp^{CF_3,CH_3}	2109	1753	1722	436	this work
Tp^{CF_3,CF_3}	2137				15c

[a] Low stability of this complex prevented acquisition of FTIR data.

and exhibits Cu−N bonds of lengths that vary significantly to yield a structure distorted from ideal C_{3v} symmetry. Thus, the Cu(1)−N(1) distance is short [1.875(5) Å], as in other Cu(I)−CH_3CN complexes,[15a,c,17] and the Cu(1)−$N_{pyrazolyl}$ distances range from 2.057(4) to 2.200(4) Å. Also contributing to the distortion from C_{3v} symmetry is the skewing of the CH_3CN axis away from the B−Cu vector.

Adoption of monomeric C_3-symmetric or fluxional lower symmetry structures for $Tp^{Ms,H}Cu(THF)$ and $Tp^{CF_3,CH_3}Cu(CH_3CN)$ in solution is indicated by ^{1}H NMR spectra in toluene-d_8 that contain sharp, single sets of the appropriate pyrazolyl and substituent resonances. The CH_3CN peak of the latter complex is broadened and shifted from that of free CH_3CN, consistent with rapid dissociation and reassociation that are common for this class of compound. Corroborating the elemental and X-ray crystallagraphic analysis, 1 equivalent of THF per copper in $Tp^{Ms,H}Cu(THF)$ was detected by ^{1}H NMR spectroscopy.[18] The ^{1}H NMR spectrum of $[Tp^{Ms,H}Cu]_x$ in toluene-d_8 closely resembles that of $Tp^{Ms,H}Cu(THF)$, implying similar fluxionality and/or structures in solution for these species. Since solutions of $[Tp^{Ms,H}Cu]_x$ and $Tp^{Ms,H}Cu(THF)$ react identically with CO and NO (vide infra), we have elected to suspend further studies aimed at comparing their solution structures.

Using an established protocol,[15b,c] the relative electronic influences of $Tp^{Ms,H}$ and Tp^{CF_3,CH_3} on a coordinated Cu(I) ion were assessed by preparing CO adducts and examining their ν(CO) values by FTIR spectroscopy (Table 3). The high value of 2109 cm^{-1} for $Tp^{CF_3,CH_3}Cu(CO)$ reflects the strong electron-withdrawing property of its scorpionate ligand, which is surpassed only by Tp^{CF_3,CF_3} [ν(CO) = 2137 cm^{-1} for its copper carbonyl complex].[15b,c] As expected, the value for $Tp^{Ms,H}$-Cu(CO) (2079 cm^{-1}) falls just below that of the $Tp^{Ph,Ph}$ analogue (2086 cm^{-1}),[15a] indicative of only minor electronic differences between these two aryl-substituted ligands. As shown in Table 3, the alkyl-substituted compounds with $Tp^{tBu,H}$ [14b] and Tp^{CH_3,CH_3} [14a] exhibit the lowest ν(CO) values and thus are the most electron rich.

Nitric Oxide Adducts. Upon addition of NO (1 atm), the colorless solution of $Tp^{Ms,H}Cu(THF)$ or $Tp^{CF_3,CH_3}Cu(CH_3CN)$ in toluene, THF, or CH_2Cl_2 immediately became orange or yellow, respectively, indicative of adduct formation (albeit not quantitative, as seen previously[6] and described below). For the $Tp^{Ms,H}$ complex, the NO adduct could be obtained as a dark orange precipitate, but NO loss from this solid was too facile to allow drying and elemental analysis. We were unable to obtain solid samples of the NO adduct in the Tp^{CF_3,CH_3} case. Both nitrosyl complexes decayed over time (vide infra), but freshly prepared solutions were amenable to spectroscopic characterization.

UV−vis spectra of the solutions generated from exposure of the Cu(I) precursors with NO contain a feature at 472 nm ($Tp^{Ms,H}$) or 436 nm (Tp^{CF_3,CH_3}) that we assign by analogy to the previously more thoroughly studied $Tp^{tBu,H}$ case as a Cu → NO MLCT transition (Table 3). For the case with Tp^{CF_3,CH_3}, we have not been able to determine an extinction coefficient because of our inability to assay the extent of NO binding; manometry results were unreliable due to decomposition of the complex in the time required for equilibration of the apparatus, and EPR and NMR methods were inapplicable (vide infra). For the $Tp^{Ms,H}$ case, by correlating ^{1}H NMR integration data obtained at 238 K that indicated ∼90% NO binding (vide infra) with UV−vis absorption intensity information under identical conditions, we estimated an extinction coefficient of 1200 ± 120 M^{-1} cm^{-1}. This absorptivity agrees well with that reported previously for $Tp^{tBu,H}Cu(NO)$ and $Tp^{Ph,Ph}Cu(NO)$ (∼1400 M^{-1} cm^{-1}).[6c] Using this extinction coefficient, we calculated that approximately 59% of $Tp^{Ms,H}Cu(THF)$ in THF binds to NO (1 atm) at 297 K. The corresponding equilibrium constant, K_{eq}, defined by eq 2, was then estimated using the extinction

$$K_{eq} = \frac{[Tp^{Ms,H}Cu(NO)]}{[Tp^{Ms,H}Cu][NO]} \quad (2)$$

coefficient and intial concentrations to calculate $[Tp^{Ms,H}Cu]$ and $[Tp^{Ms,H}Cu(NO)]$ and determining [NO] in THF through extrapolation of solubility data in the literature for cyclohexane.[19] At 297 K, K_{eq} = 85 ± 25 M^{-1}, with the large estimated error arising from the inexact extinction coefficient and NO concentration values. A similar value of K_{eq} = 140 ± 10 M^{-1} was reported previously for NO binding to $[Tp^{tBu,H}Cu]_2$ in toluene at 296 K.[6c]

Consistent with the MLCT assignment for the optical absorption feature of the nitrosyl adducts, as the electron-withdrawing capability of the $Tp^{R,R'}$ ligand and the ν(CO) value for its Cu(I)−CO complex increase down the series listed in Table 3, so does the energy of the absorption band of the nitrosyl complex. The relative electron-withdrawing influences of the $Tp^{R,R'}$ ligands are also reflected by the ν(NO) values in the FTIR spectra, which were identified as nitrosyl stretches by their ^{15}NO isotope shifts that matched those calculated theoretically for a NO harmonic oscillator [Table 3; observed ν(^{14}NO)/ν(^{15}NO) = 1.018−1.020; calculated = 1.019].

Surprisingly, the solutions obtained upon reactions of NO with $Tp^{Ms,H}Cu(THF)$ and $Tp^{CF_3,CH_3}Cu(CH_3CN)$ were EPR silent between room temperature and 4.2 K; only signals corresponding to free NO plus Cu(II) impurities that integrated for <10% of the available copper in the samples were observed at 4.2 K. This lack of an EPR signal stands in distinct contrast to the cases of the nitrosyl adducts formed in Cu−zeolites and of those supported by $Tp^{tBu,H}$ and $Tp^{Ph,Ph}$, which exhibit characteristic signals with g < 2.0 and large Cu and NO hyperfine splitting.[5,6] We did note that the color of the solutions deepened considerably upon freezing, suggestive of a chemical change (dimerization or binding of a second NO molecule?)[20] that might result in loss of EPR activity. Unfortunately, the ^{1}H NMR spectrum of $Tp^{CF_3,CH_3}Cu(CH_3CN)$ under 1 atm of NO in THF-d_8 only shows Cu(I) starting material between 213 K and room

(17) But see: Tyeklar, Z.; Jacobson, R. R.; Wei, N.; Murthy, N. N.; Zubieta, J.; Karlin, K. D. *J. Am. Chem. Soc.* **1993**, *115*, 2677−2689.

(18) Due to a long T_1 of 26 s for the THF hydrogens (measured by the inversion recovery method), observation of full intensity for the THF signal necessitated using a relaxation delay time of ∼90 s in the FT-NMR experiment.

(19) (a) Tsiklis, D. S.; Svetlova, G. M. *Zh. Fiz. Khim.* **1958**, *32*, 1476−1480. (b) *Solubility Data Series: Oxides of Nitrogen*; Young, C. L., Ed.; Pergamon Press: Oxford, U.K., 1981; Vol. 8.

(20) UV−vis or FTIR data acquired at cryogenic temperatures (<77 K) would be informative, but we have been unable to make these measurements.

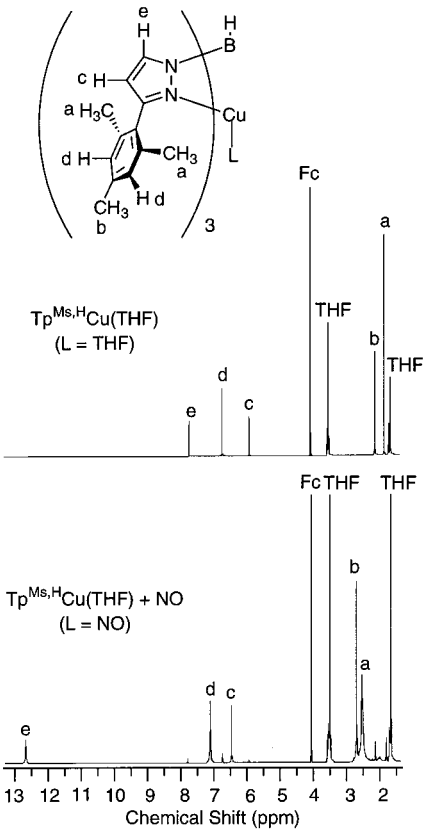

Figure 4. ^{1}H NMR spectra (THF-d_8, 238 K, 300 MHz) with peak assignments of (top) $Tp^{Ms,H}Cu(THF)$ and (bottom) $Tp^{Ms,H}Cu(THF)$ + NO (1 atm).

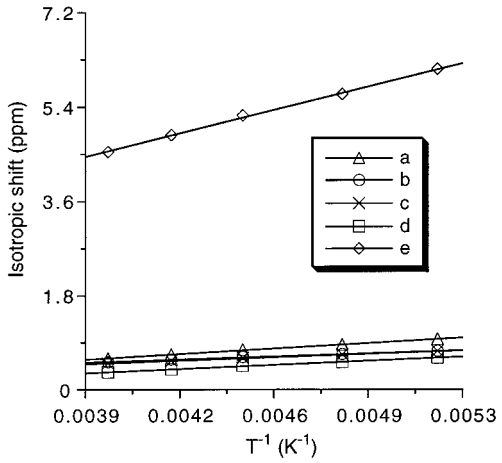

Figure 5. Temperature dependence of isotropic shifts for $Tp^{Ms,H}CuNO$ (peak assignments as shown in Figure 4).

Table 4. Nuclear Relaxation Rates and Estimated N(nitrosyl)···H Distances (r) for $Tp^{Ms,H}CuNO$

hydrogens[a]	T_{1M} (s)[b]	T_{2M} (s)[c]	r (Å)[d]
a	0.027(2)	0.019	4.9(11)
b	0.21(2)	0.069	6.0(8)
c	0.29(4)	0.065	6.3(2)
d	0.080(8)	0.038	5.0(3)
e	0.38(4)	0.050	6.6(2)

[a] Labels refer to assignments indicated in Figure 4. [b] Measured using the inversion recovery method at 223 K (500 MHz). Estimated standard deviations are given in parentheses. [c] Measured from the peak width at half-height. [d] Estimated by superimposing the coordinates for the CuNO fragment from the X-ray structure of $Tp^{tBu,H}CuNO$[6c] on those from the structure of $Tp^{Ms,H}Cu(THF)$.

temperature, similar to the spectra of the EPR-active $Tp^{tBu,H}$ and $Tp^{Ph,Ph}$ systems.[6] Thus, it seems that the chemical changes at the low temperatures (<40 K) required to observe an EPR signal[6] in conjunction with paramagnetic properties that preclude observation of NMR data (e.g., a long electron relaxation correlation time, τ_s) at high temperatures (>200 K) conspire to prevent further EPR and NMR spectroscopic characterization of $Tp^{CF_3,CH_3}Cu(NO)$.[21]

However, the ^{1}H NMR spectrum of $Tp^{Ms,H}Cu(THF)$ in THF-d_8 under 1 atm of NO at 238 K (temperature chosen to increase NO binding and inhibit decomposition; vide infra) contained a new set of peaks along with those of the Cu(I) starting material in an ~9:1 ratio (Figure 4). By a comparison of the peak intensities to those of the added ferrocene standard, ≥95% of the $Tp^{Ms,H}$ present in the sample was accounted for by these two sets of signals. The number of peaks for the major species under NO indicates that it is effectively C_3-symmetric, with equivalent environments for the substituted pyrazolyl groups. The peak positions and widths indicate the influence of a paramagnetic center. The presence of peaks due to $Tp^{Ms,H}Cu(THF)$ in addition to those due to the major species rules out nonspecific effects of free NO in solution on the NMR properties of $Tp^{Ms,H}Cu(THF)$ as being responsible for the new signals. Moreover, dynamic equilibration between $Tp^{Ms,H}Cu(THF)$ and the major species was indicated by saturation transfer experiments, wherein saturation of the 5′-pyrazolyl hydrogen signal of $Tp^{Ms,H}Cu(THF)$ at 7.7 ppm caused loss of intensity of the most downfield resonance at 12.6 ppm of the major species under NO. This result also allowed assignment of the 12.6 ppm peak to the 5′-pyrazolyl hydrogen in the major species. Thus, we ascribe the ^{1}H NMR spectrum of $Tp^{Ms,H}Cu(THF)$ under NO to paramagnetic $Tp^{Ms,H}Cu(NO)$ (major) in equilibrium with the starting Cu(I) complex (minor). Evidently, the electron relaxation correlation time (τ_s) for the nitrosyl supported by $Tp^{Ms,H}$ (NMR active) is shortened compared to those of the $Tp^{tBu,H}$ and $Tp^{Ph,Ph}$ complexes (EPR active, albeit only at temperatures <40 K).[6]

The indicated peak assignments for $Tp^{Ms,H}Cu(NO)$ were deduced from integrated intensities, isotropic shifts and their temperature dependencies (Figure 5), and the nuclear relaxation rates (Table 4). Also listed in Table 4 are approximate distances (r) between the $Tp^{Ms,H}$ hydrogens and the unpaired spin, which was assumed to be localized on the nitrosyl nitrogen. Because the SOMO has a large component on N, this is a reasonable qualitative assumption based on theory,[6c] but a more sophisticated treatment should take into account delocalization of the electron over the entire CuNO unit. The distances r (averaged over chemically equivalent hydrogen nuclei) were estimated by superimposing the CuNO core coordinates determined by X-ray crystallography[6c] for $Tp^{tBu,H}Cu(NO)$ on those for the $Tp^{Ms,H}Cu$ fragment from the X-ray structure of $Tp^{Ms,H}Cu(THF)$. The nuclear relaxation rates T_{1M} and T_{2M} were measured at 223 K by using the inversion recovery method and the line width at half-height, respectively (Table 4).[22] Consistent with a dominant

(21) We also have been frustrated in our attempts to obtain an EPR signal for $Tp^{CH_3,CH_3}Cu(NO)$, but for different reasons. It disproportionates to $Tp^{CH_3,CH_3}Cu(NO_2)$ and N_2O very rapidly, about as fast as it is formed. As a result, we have been unable to avoid a large Cu(II) signal due to $Tp^{CH_3,CH_3}Cu(NO_2)$ that overwhelms the EPR spectrum and prevents observation of the nitrosyl complex signal in this case.

(22) The absolute T_{2M} values are not necessarily accurate, as the relatively narrow line widths observed render the method used to obtain them suspect (see pp 253−254 in ref 23). Still, it is worth considering the relative magnitudes of the estimated T_{2M} values listed in Table 4, which follow the trends for the T_{1M} values.

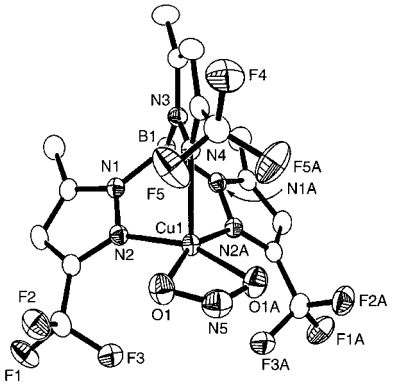

Figure 6. Representation of the X-ray crystal structure of Tp^{CF_3,CH_3}-$Cu(NO_2)$ (50% ellipsoids; hydrogen atoms omitted for clarity; heteroatoms labeled).

dipolar contribution to the relaxation of the hydrogen nuclei, T_{1M} tracks approximately with r^{-6},[23] but there is significant scatter about a linear fit to a plot of T_{1M}^{-1} versus r^{-6}. We attribute this poor fit to the spread of hydrogen positions for each chemically equivalent site and error inherent in the assumption of spin localization on N in the CuNO unit. As is evident from Figure 5, the 5′-pyrazolyl hydrogen most distant from the paramagnetic locus exhibits the largest isotropic shift with the greatest temperature dependence, with much smaller shifts evident for all of the other hydrogen atoms. These results implicate the dominance of a contact interaction between the 5′-pyrazolyl hydrogen and the unpaired spin, presumably via a σ and/or π delocalization mechanism.[23] Much weaker contact and/or dipolar interactions apparently are responsible for the smaller isotropic shifts for the other hydrogen atoms in the ligand. The orthogonality of the pyrazolyl and mesityl rings coupled with the large number of bonds separating the mesityl hydrogens from the paramagnetic center would attenuate σ or π delocalization onto them, consistent with their small isotropic shifts.

Disproportionation Reactivity. Like the NO adducts supported by $Tp^{Ph,Ph}$ and Tp^{CH_3,CH_3},[6d] the nitrosyls $Tp^{Ms,H}Cu(NO)$ and $Tp^{CF_3,CH_3}Cu(NO)$ decompose under excess NO to yield N_2O and the respective Cu(II)−nitrite complex $Tp^{R,R'}Cu(NO_2)$. Production of 0.6−1.0 equiv (based on Cu) of N_2O was confirmed by GC analysis of the headspace gases. In situ UV−vis or EPR monitoring of the reactions revealed quantitative generation of $Tp^{CF_3,CH_3}Cu(NO_2)$ or $Tp^{Ms,H}Cu(NO_2)$; these products also were isolated from the reaction mixtures as crystalline solids in 62% and quantitative yields, respectively. In addition, $Tp^{Ms,H}Cu(NO_2)$ was prepared independently via admixture of $TlTp^{Ms,H}$, $CuCl_2$, and $NaNO_2$. Identification of this compound rested on its proper elemental analysis, spectroscopic features consistent with a mononuclear 5-coordinate Cu(II) complex [UV−vis λ (ϵ) 300 (1500 M^{-1} cm^{-1}), 390 (sh, 260), 778 (70) nm; EPR (9.47 GHz, 77 K) $g_{||} = 2.31$, $g_{\perp} = 2.06$, $A_{||}^{Cu} = 135$ G, $A_{||}^{N} = 10$ G, $A_{\perp}^{N} = 12$ G], and NO_2^- ligand vibrations in the FTIR spectrum that shifted appropriately when $^{15}NO_2^-$ was incorporated. Analogous analytical and spectral data were obtained for $Tp^{CF_3,CH_3}Cu(NO_2)$, which also was characterized by an X-ray crystal structure (Figure 6 and Tables 1 and 2).

The topology of $Tp^{CF_3,CH_3}Cu(NO_2)$ is analogous to that of its Tp^{CH_3,CH_3} analogue reported previously[6d] but differs from that of $Tp^{tBu,H}Cu(NO_2)$.[24] Both of the Tp^{CF_3,CH_3} and Tp^{CH_3,CH_3} compounds contain square pyramidal Cu(II) ions with a symmetrically coordinated nitrite ion *O*,*O*-bound in the basal plane. In contrast, the Cu(II) geometry in the $Tp^{tBu,H}$ complex is distorted trigonal bipyramidal and the Cu(II)−$O_{nitrite}$ bond distances differ considerably [1.976(5) and 2.169(6) Å]. These structural differences have spectral consequences; most notably, the Tp^{CF_3,CH_3} and Tp^{CH_3,CH_3} compounds exhibit quite similar axial EPR signals[6d] but the signal for the $Tp^{tBu,H}$ complex is rhombic.[24] Overall, the analogous properties of the Cu(II)−NO_2^- complexes supported by Tp^{CF_3,CH_3} and Tp^{CH_3,CH_3} are consistent with similar steric effects for these two scorpionates, with the large *tert*-butyl substituents in $Tp^{tBu,H}Cu(NO_2)$ being responsible for its divergent structural and spectral features.

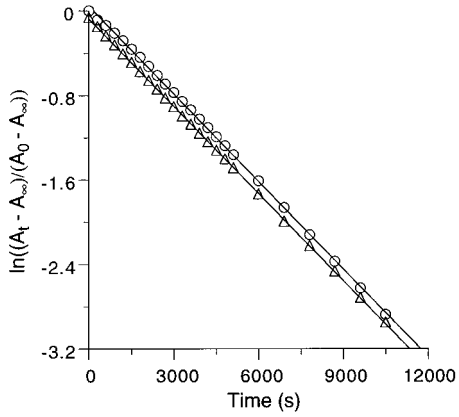

Figure 7. Representative pseudo-first-order plot of kinetic data for the loss of TpMs,HCuNO (○) and the formation of $Tp^{Ms,H}Cu(NO_2)$ (△) under 1.5 atm of NO(g) at 297 K. Linear fits to the data are shown, with slopes corresponding to $k_{obs1} = 2.76(2) \times 10^{-4}$ s^{-1} ($R = 0.9998$) and $k_{obs2} = 2.75(2) \times 10^{-4}$ s^{-1} ($R = 0.9999$).

Table 5. NO Disproportionation Rate Constants for the Decay of $Tp^{R,R'}CuNO$ (k_{obs1}) and the Formation of $Tp^{R,R'}Cu(NO_2)$ (k_{obs2})[a]

ligand	$10^4 k_{obs1}$ (s^{-1})[4]	k_{obs2} (s^{-1})	ref
Tp^{CH_3,CH_3}	>30[b]	>30[b]	6d
$Tp^{Ms,H}$ [d]	3.9(2)	3.9(1)	this work
$Tp^{Ph,Ph}$	2.0(1)	1.8(1)	[c]
Tp^{CF_3,CH_3}	0.65(3)	0.40(3)	this work
$Tp^{tBu,H}$	<0.16[e]	<0.16[e]	6c

[a] Conditions: 2 atm of NO(g), 297 K, CH_2Cl_2. Estimated standard deviations are indicated in parentheses. [b] Estimated from data previously reported using different NO pressures. [c] Ruggiero, C. E. Ph.D. Thesis, University of Minnesota, 1995. [d] In THF. [e] Upper bound estimated from observed stability of $Tp^{tBu,H}Cu(NO)$; N_2O generation not confirmed.

The rates of disproportionation of $Tp^{Ms,H}Cu(NO)$ and Tp^{CF_3,CH_3}-$Cu(NO)$ were measured by monitoring the decay of the Cu → NO MLCT band and/or the growth of the d → d absorption feature of the product nitrite complex under conditions of excess NO. First-order plots of the data over 1−6 half-lives were linear ($R > 0.997$; for a representative plot, see Figure 7), providing observed rate constants for nitrosyl complex decay (k_{obs1}) and nitrite complex production (k_{obs2}). The rate constants obtained under 2.0 atm of NO are listed with the values obtained previously[6d] for the Tp^{CH_3,CH_3}, $Tp^{Ph,Ph}$, and $Tp^{tBu,H}$ systems in Table 5. The k_{obs1} and k_{obs2} values for each run generally were the same within experimental error. However, in some instances $k_{obs1} \neq k_{obs2}$, particularly for the Tp^{CF_3,CH_3} case at low NO pressure, indicative of a metastable intermediate (yet to be observed by spectroscopy) or possible mass transfer effects (diffusion of gas into solution) under these particular conditions. Both steric and electronic effects on the rate of NO disproportionation are evident from the data in Table 5. Particularly illustrative comparisons are (a) the different rates for the

(23) Bertini, I.; Luchinat, C. In *NMR of Paramagnetic Substances*; Lever, A. B. P., Ed.; Coordination Chemistry Reviews, Vol. 150; Elsevier: New York, 1996.

(24) Tolman, W. B. *Inorg. Chem.* **1991**, *30*, 4878−4880.

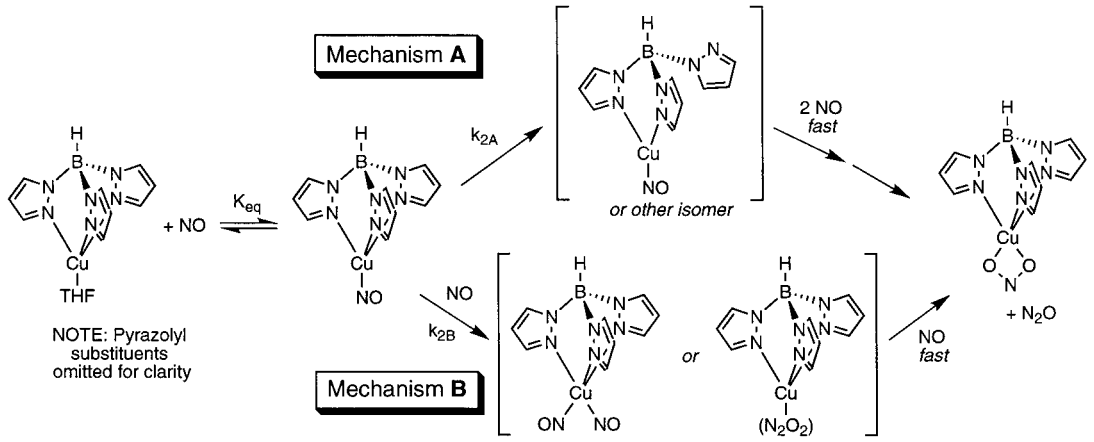

Figure 8. Proposed mechanisms for the disproportionation of nitric oxide mediated by $Tp^{R,R'}Cu^{I}$ complexes.

electronically similar systems with the sterically hindered $Tp^{tBu,H}$ (slow) and much less hindered Tp^{CH_3,CH_3} (fast) and (b) the different rates for the compounds supported by the similarly sized but relatively electron-donating Tp^{CH_3,CH_3} (fast) and electron-withdrawing Tp^{CF_3,CH_3} (slow).

Shown in Figure 8 are the two simplest mechanisms that would account for (a) the existence of a rapid equilibrium between the Cu(I) precursor and its NO adduct (K_{eq}, eq 2) and (b) the observed first-order dependence of the disproportionation rate on the copper complex concentration. In pathway A, equilibration between the starting Cu(I) complex and its NO adduct is followed by some type of rate-determining unimolecular isomerization (k_{2A}). Loss of a pyrazolyl arm of the scorpionate ligand is one attractive possibility, as such arm dissociation/reassociation paths have been identified in other reactions of Tp complexes.[14b,25] Subsequent fast and kinetically invisible steps involving binding of a second NO molecule, N−N bond formation, and oxygen atom transfer would ensue. The rate law for mechanism A is described by eqs 3 and 4,

$$\text{rate} = k_{obs}[Cu_{tot}] \tag{3}$$

$$k_{obs} = \frac{k_2 K_{eq}[NO]}{1 + K_{eq}[NO]} \tag{4}$$

where $[Cu_{tot}] = [TpCu(THF)] + [TpCu(NO)]$ (for derivations, see Supporting Information). The alternative pathway B differs only by virtue of the rate-controlling step, which here involves attack at the nitrosyl adduct by a second NO molecule, either at bound NO or at Cu, to yield a *cis*-dinitrosyl or a hyponitrite species, respectively, in a bimolecular step (k_{2B}). Again, the final products, N_2O and $Tp^{R,R'}Cu(NO_2)$, would then be generated in subsequent fast and ill-defined steps. The expression for k_{obs} for mechanism B is given by eq 5.

$$k_{obs} = \frac{k_2 K_{eq}[NO]^2}{1 + K_{eq}[NO]} \tag{5}$$

Comparison of eqs 4 and 5 indicates differences in the dependence on the concentration of NO for mechanisms A and B, suggesting that they may be distinguished experimentally by measuring k_{obs} as a function of [NO]. We performed the experiments for the $Tp^{Ms,H}$ case, as these were facilitated by the close correspondence between k_{obs1} and k_{obs2} combined with the convenient rates at room temperature. The disproportionation rate constant was found to be dependent on the NO pressure (509−1500 Torr) as shown in Figure 9. Here, $k_{obs1}(1 + K_{eq}[NO])/K_{eq}$ (see eqs 4 and 5) is plotted versus [NO] (Figure 9a) and $[NO]^2$ (Figure 9b), where k_{obs1} is multiply determined for three to nine runs at each NO pressure, and the K_{eq} value is

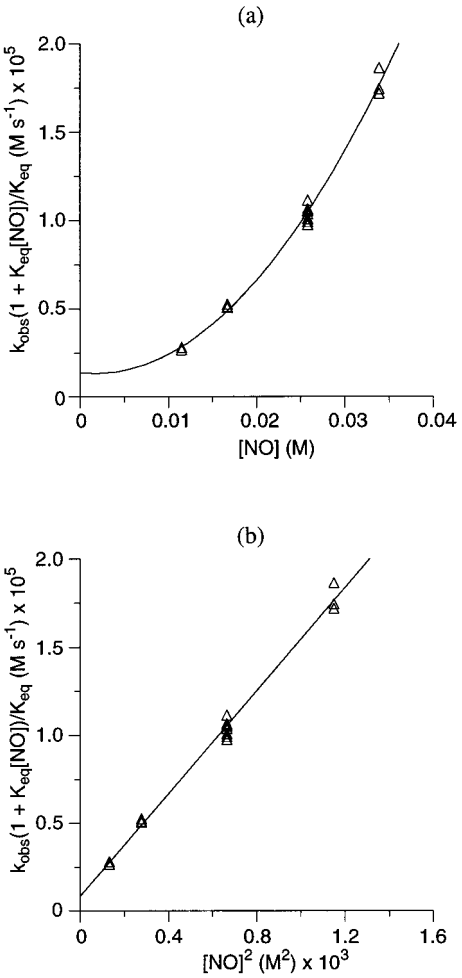

Figure 9. Plots of $k_{obs1}(1 + K_{eq}[NO])/K_{eq}$ versus [NO] (a) and $[NO]^2$ (b) for the NO disproportionation reaction mediated by $Tp^{Ms,H}CuNO$, where K_{eq} is that determined from NMR and UV−vis measurements (85 ± 25 M^{-1}). In (a), the parabola is a fit of the data to a second-order polynomial ($y = a + bx + cx^2$; $a = 1.38 \times 10^{-6}$, $b = -5.4 \times 10^{-5}$, $c = k_2 = 0.0158(5)$ s^{-1}; $R = 0.996$). In (b), a linear fit is shown ($R = 0.996$; slope $= k_2 = 0.0146(5)$ s^{-1}).

(25) (a) Bucher, U. E.; Currao, A.; Nesper, R.; Rüegger, H.; Venanzi, L. M.; Younger, E. *Inorg. Chem.* **1995**, *34*, 66−74. (b) Looney, A.; Parkin, G. *Polyhedron* **1990**, *9*, 265−276. (c) Keyes, M. C.; Young, V. G., Jr.; Tolman, W. B. *Organometallics* **1996**, *15*, 4133−4140.

that determined from NMR and UV−vis measurements (85 ± 25 M^{-1}). The good fits of the data in Figure 9a (vs [NO]) to a parabola [$y = a + bx + cx^2$, $c = k_2 = 0.0158(5)$ s^{-1}; $R = 0.996$] and in Figure 9b (vs $[NO]^2$) to a straight line [slope = $k_2 = 0.0146(5)$ s^{-1}; $R = 0.996$] are strong evidence in support of eq 5 (mechanism B) and argue against eq 4 (mechanism A).[26] Similar results also were obtained for $Tp^{Ph,Ph}$ (data not shown). Thus, the data best support the pathway wherein reaction of NO with $Tp^{R,R'}Cu(NO)$ occurs in the rate-determining step.

Discussion

Nitric oxide reacts with the copper(I) complexes $Tp^{Ms,H}$-Cu(THF) and $Tp^{CF_3,CH_3}Cu(CH_3CN)$ to yield mononuclear mononitrosyl adducts, identified as such principally on the basis of optical and infrared absorption features and disproportionation reactivity analogous to that previously identified for structurally defined $Tp^{tBu,H}Cu(NO)$ (Figure 1) and congeners supported by $Tp^{Ph,Ph}$ and Tp^{CH_3,CH_3}.[6] Thus, each member of the set of $Tp^{R,R'}$-Cu(NO) species exhibits a Cu → NO MLCT band with λ_{max} = 430−500 nm ($\epsilon \sim 1200$ M^{-1} cm^{-1}) and a single ν(NO) between 1712 and 1753 cm^{-1} that shifts appropriately upon substitution with ^{15}NO (Table 3). In addition, all of the adducts, except the most stable one supported by $Tp^{tBu,H}$, react further with NO to yield N_2O and the respective nitrite complex $Tp^{R,R'}Cu(NO_2)$. These important similarities in spectral properties and reactivity allow the nitrosyl complexes of the various $Tp^{R,R'}$ ligands to be identified as constituents of a topologically analogous class comprising the novel $\{CuNO\}^{11}$ unit. Despite these similarities that provide convincing evidence of structural congruence, however, the different substituents on the various $Tp^{R,R'}$ scaffolds induce significant disparities in key properties of the nitrosyl complexes, as illustrated in particular by the studies of the $Tp^{Ms,H}$ and Tp^{CF_3,CH_3} cases reported herein.

The X-ray structures of $Tp^{Ms,H}Cu(THF)$ (Figure 2) and of other reported complexes of the $Tp^{Ms,H}$ ligand[12] show that it provides a relatively rigid cavity of defined shape, lined by arene groups, about the remaining substrate binding site. The phenyl substituents in the related ligand $Tp^{Ph,Ph}$ afford a less well-defined binding pocket of different effective shape due to the ability of the phenyl groups to rotate about the C−C bond connecting them to their respective pyrazolyl groups.[14b] Not surprisingly, electronic differences between $Tp^{Ms,H}$ and $Tp^{Ph,Ph}$ are insignificant, as shown by the similar CO and NO stretching frequencies and MLCT energies in the respective copper adducts (Table 3). A large effect on the NO disproportionation rate due to the different substituent environments of these two ligands is also absent (Table 5), further supporting the notion that steric and electronic disparities between them are subtle. However, while previous work showed that $Tp^{Ph,Ph}Cu(NO)$ exhibits a distinct EPR signal below 40 K with $g < 2.0$ and large NO hyperfine splitting features like that of $Tp^{tBu,H}Cu(NO)$,[6] here we report that the $Tp^{Ms,H}$ analogue is EPR silent at 4.2 K and exhibits a sharp NMR spectrum (at 238 K) perturbed (albeit relatively slightly) by the paramagnetism arising from the unpaired spin density of the $\{CuNO\}^{11}$ core. We hypothesize that the distinctly contrasting spectroscopic behavior derives from a shortening of the electron spin correlation time, τ_s, of the $Tp^{Ms,H}$ complex compared to that supported by $Tp^{Ph,Ph}$.[23] This shorter τ_s renders $Tp^{Ms,H}Cu(NO)$ amenable to NMR characterization. Although it is difficult to ascertain the cause of the short τ_s value, we speculate that relaxation in the $Tp^{Ms,H}$ case is enhanced by an Orbach process involving low-lying excited states.[27] Perhaps this process is promoted by interactions of the bound NO with the π electron systems of the specifically oriented aromatic rings enclosing the $Tp^{Ms,H}$ binding pocket. Whatever the specific rationale, the finding that a simple perturbation of aromatic ring geometry surrounding the bound NO in the $Tp^{Ph,Ph}$ and $Tp^{Ms,H}$ complexes induces a drastic change in the EPR and NMR properties is significant, with particular implications for spectroscopic studies of $\{CuNO\}^{11}$ adducts in zeolites and proteins. Thus, care should be exercised in characterizing such adducts, as subtle environmental effects may determine the applicability of EPR versus NMR methods.

Whereas unique EPR and NMR properties are observed for $Tp^{Ms,H}Cu(NO)$ due to its specifically shaped substrate binding pocket, the electron-withdrawing influences of the trifluoromethyl substituents of Tp^{CF_3,CH_3} are dominant in affecting other properties of its complexes.[11] The electron-withdrawing effect of Tp^{CF_3,CH_3} is manifested clearly by high ν(CO) and ν(NO) values for its respective copper carbonyl and nitrosyl complexes and a short λ_{max} for the Cu → NO MLCT feature for the latter (Table 3). Consideration of the similar structures of the copper-(II)−nitrite complexes supported by Tp^{CF_3,CH_3} (Figure 6) and Tp^{CH_3,CH_3} [6d] supports comparable effective sizes for the binding pockets of these ligands, the substituents of the former being only slightly larger than the latter. While steric factors influence the rate of NO disproportionation by the copper complexes of the $Tp^{R,R'}$ ligands (Table 5), the large difference in k_{obs} values for the similarly sized Tp^{CF_3,CH_3} and Tp^{CH_3,CH_3} cases (>45-fold) implicates a significant electronic effect as well. In other words, the experimental data show that increased steric hindrance and electron withdrawal by the supporting ligand slow the NO disproportionation rate considerably. Consistent with this result, mechanistic studies show that attack of a second, electrophilic NO molecule on the initially and reversibly formed mono-copper−mononitrosyl adduct is rate-controlling (mechanism B, Figure 8). These findings also have implications in protein- and zeolite-based Cu/NO reactions wherein multiple NO decomposition pathways may compete.[3−5] Extrapolation of our results to these systems suggests that disproportionation of NO to N_2O and NO_2^- would be disfavored in an electron-poor environment (e.g., such as in the oxygen-rich zeolites).

Conclusions

Copper(I) complexes of $Tp^{Ms,H}$ and Tp^{CF_3,CH_3} have been characterized and their reactions with NO explored. Mono-copper−mononitrosyl adducts form in both cases, as shown by spectroscopic comparisons to previously prepared examples.[6] However, these studies also reveal significant effects on the spectroscopy and reactivity of the $\{CuNO\}^{11}$ unit that arise from the substituents on $Tp^{Ms,H}$ and Tp^{CF_3,CH_3}. Thus, in contrast to its relative coordinated to $Tp^{Ph,Ph}$ that is EPR active and not amenable to NMR characterization, the nitrosyl complex supported by $Tp^{Ms,H}$ exhibits a sharp ^1H NMR spectrum. Notwithstanding our lack of a definitive rationale for this unique

(26) If rate law 4 for mechanism A were operative, the plot in Figure 9a would be linear and that in Figure 9b would be parabolic. Although the data may be fit accordingly ($R = 0.98$ for linear fit of Figure 9a and $R = 0.996$ for parabolic fit of Figure 9b), the associated k_2 values for these fits (which should be identical) differ by more than 3 orders of magnitude [6.5×10^{-4} s^{-1} vs 0.77 s^{-1}, respectively]. Thus, the combination of better fits of Figure 9a and Figure 9b to a parabola and a straight line, respectively ($R = 0.996$), *and* the close agreement between the associated k_2 values [$0.0146(5)$ s^{-1} vs $0.0158(5)$ s^{-1}] better supports rate law 5 and mechanism B. While it would be preferable to corroborate this conclusion using data obtained at high NO pressures near the saturation limit, this has not been experimentally feasible to date (NO pressures ~ 7000 Torr would be needed to increase [NO] sufficiently to make $K_{eq}[NO] \gg 1$).

(27) (a) Orbach, R. *Proc. R. Soc. London, Ser. A* **1961**, *264*, 458. (b) See pp 83−88 in ref 23.

spectral behavior, the discovery that a subtle difference in the binding pocket provided by the two arene-substituted ligands induces a drastic change in the applicable spectroscopic method has important implications for studies of copper nitrosyls in catalytic and biological systems. The electron-poor nature of Tp^{CF_3,CH_3} is reflected in the spectral features of its copper−carbonyl and −nitrosyl adducts and results in a significant slowing of the rate of disproportionation of the latter to N_2O and $Tp^{CF_3,CH_3}Cu(NO_2)$. Consistent with this electronic effect and a rate decrease with increased steric bulk in electronically similar systems, mechanistic studies support a mechanism for the disproportionation reaction involving preequilibration of NO and the Cu(I) precursor with the CuNO adduct, followed by rate-determining electrophilic attack of a second NO molecule. Overall, the results reported herein of studies of the $Tp^{Ms,H}$ and Tp^{CF_3,CH_3} systems illustrate the importance of the specific ligand environment in affecting copper−nitrosyl complex properties.

Experimental Section

General Procedures. Unless otherwise noted, all reagents, solvents, and gases used were obtained commercially and were of analytical grade. When necessary, solvents were dried according to published procedures[28] and distilled under N_2 immediately prior to use. Nitric oxide gas was purified according to published procedures.[6c] ^{15}NO was purchased from Cambridge Isotope Laboratories, Inc., and used without further purification. All air-sensitive reactions were performed either in a Vacuum Atmospheres inert-atmosphere glovebox under a N_2 atmosphere or by using standard Schlenk and vacuum-line techniques. The compounds $TlTp^{Ms,H}$,[12] $NaTp^{CF_3,CH_3}$,[11] and $[Cu(CH_3CN)_4]SbF_6$[29] were prepared according to published procedures. Cuprous chloride was purchased from Mallinckrodt, purified by published procedures,[28] and stored under N_2. Elemental analyses were performed by Atlantic Microlabs, Norcross, GA. Spectroscopic and GC/MS data were collected as described previously.[6c,30] Analyses of N_2O evolution by gas chromatography were performed on a Hewlett-Packard 5890 Series II gas chromatograph with a HP 3396 Series II integrator and a Poropak Q column (6 ft, 15 mL/min flow rate, 293 K, He carrier gas).

3-(Trifluoromethyl)-5-methylpyrazole. This method combines steps similar to those used to prepare 3,5-bis(trifluoromethyl)pyrazole.[31] 1,1,1-Trifluoropentane-2,4-dione (10.0 g, 0.0649 mol) was dissolved under N_2 in degassed absolute EtOH (90 mL), and the solution was cooled to 273 K. Hydrazine monohydrate (3.9 g, 0.0779 mol) was added via syringe over 10 min, and the mixture was stirred for ∼2 h at 273 K. Most of the solvent was removed under reduced pressure to leave a thick white slurry. The slurry was dissolved in dry, degassed benzene (200 mL), and the solution was then refluxed for 2 d through a thimble filled with calcium hydride. Most of the benzene was removed by distillation under nitrogen, with the last ∼30 mL removed under reduced pressure without heating to prevent charring of the product. The remaining white residue was then sublimed under vacuum (0.05 Torr) through bent glass tubing using a heat gun to separate evolved H_2O from the sublimate. The product was then collected as a white solid (8.4 g, 86%). GC/MS: t_R 5.91 min, *m*/*z* (relative intensity) 150 (100, M^+). ^1H NMR data matched those reported previously.[32]

$Tp^{CF_3,CH_3}CuCH_3CN$. $[Cu(CH_3CN)_4]SbF_6$ (0.530 g, 1.14 mmol) was dissolved under nitrogen in dry, degassed THF (8 mL). $NaTp^{CF_3,CH_3}$ (0.550 g, 1.14 mmol) dissolved in THF (8 mL) was added. After 2−3 h of stirring at room temperature, the solvent was removed under reduced pressure. The off-white residue was slurried in CH_2Cl_2 (∼20 mL), the slurry was filtered through Celite, and the filtrate was concentrated to about 5−10 mL. Slow evaporation under N_2 yielded colorless crystals suitable for X-ray diffraction analysis (0.530 g, 83%): ^1H NMR (300 MHz, CD_2Cl_2) δ 2.23 (s, 3 H), 2.45 (s, 9 H), 6.25 (s, 3 H) ppm; $^{13}C\{^1H\}$ NMR (75 MHz, CD_2Cl_2) δ 2.2, 12.3, 103, 121.5 (q, $J_{C,F}$ = 269 Hz), 141.1 (q, $J_{C,F}$ = 37 Hz), 145 ppm; FTIR (KBr) 2558 [ν(BH)], 2277, 1609, 1496, 1461, 1356, 1244, 1188, 1131, 1068, 998, 808, 786, 744, 646 cm^{-1}. Anal. Calcd for $C_{17}H_{16}N_7CuBF_9$: C, 36.22; H, 2.86; N, 17.39. Found: C, 36.73; H, 2.92; N, 17.65.

$Tp^{Ms,H}Cu(THF)$. $TlTp^{Ms,H}$ (1.029 g, 1.33 mmol) and cuprous chloride (0.145 g, 1.46 mmol) were stirred in THF (15 mL) for 10 min. The solution then was filtered, the volume was reduced under vacuum to 5 mL, and pentane was allowed to diffuse into the solution at 253 K to give the product as colorless crystals suitable for X-ray diffraction analysis (0.490 g, 52%): ^1H NMR (500 MHz, toluene-d_8, 216 K) δ 1.38 (m, 4 H), 2.12 (s, 18 H), 2.15 (s, 9 H), 3.58 (m, 4 H), 5.87 (d, J = 2.0 Hz, 3 H), 6.77 (s, 6 H), 7.63 (d, J = 2.0 Hz, 3 H) ppm; $^{13}C\{^1H\}$ NMR (75 MHz, CD_2Cl_2) δ 20.59, 21.45, 26.13, 68.31, 106.69, 128.39, 130.73, 136.44, 137.72, 137.86, 153.07 ppm; FTIR (KBr) 2960, 2953, 2916, 2420 [ν(BH)], 1478, 1461, 1345, 1179, 1165, 1033, 771, 743, 709 cm^{-1}. Anal. Calcd for $C_{36}H_{40}N_6BCu$: C, 68.32; H, 6.88; N, 11.95. Found: C, 68.62; H, 6.84; N, 12.13.

$[Tp^{Ms,H}Cu]_x$. This complex was obtained either by recrystallizing $Tp^{Ms,H}Cu(THF)$ via diffusion of pentante into a toluene solution (23% yield) or by drying $Tp^{Ms,H}Cu(THF)$ under vacuum (95% yield): ^1H NMR (500 MHz, toluene-d_8, 213 K) δ 2.04 (s, 18 H), 2.16 (s, 9 H), 5.85 (d, J = 2.0 Hz, 3 H), 6.79 (s, 6 H), 7.64 (d, J = 2.0 Hz, 3 H) ppm; $^{13}C\{^1H\}$ NMR (125 MHz, benzene-d_6) δ 20.3, 20.8, 104.5, 127.9, 132.2, 135.1, 137.2, 137.8, 151.1 ppm; FTIR (KBr) 2972, 2918, 2386 [ν(BH)], 1613, 1486, 1461, 1351, 1200, 1184, 1165, 1071, 1037, 847, 788, 734, 711 cm^{-1}. Anal. Calcd for $C_{36}H_{40}N_6BCu$: C, 68.51; H, 6.39; N, 13.32. Found: C, 68.85; H, 6.50; N, 13.39.

$Tp^{CF_3,CH_3}CuCO$. $Tp^{CF_3,CH_3}Cu(CH_3CN)$ (0.054 g, 0.096 mmol) was dissolved under N_2 in dry, degassed CH_2Cl_2 (2 mL), and the solution was cooled to 263 K. CO gas was bubbled through the solution for ∼5 min. After the solution was warmed to room temperature under a CO purge, the Schlenk flask was sealed and the reaction mixture was stirred for an additional 30 min. The solvent was removed under reduced pressure, the off-white residue was redissolved in CH_2Cl_2, and pentane was allowed to diffuse into the solution at room temperature to yield the product as a white crystalline solid (53 mg, 100%): ^1H NMR (300 MHz, CD_2Cl_2) δ 2.46 (s, 9 H), 6.32 (s, 3 H); $^{13}C\{^1H\}$ NMR (75 MHz, THF-d_8) δ 12.5, 105.2, 122.4 (q, $J_{C,F}$ = 268 Hz), 143.2, 147.2, 168.7 ppm; FTIR (KBr) 2558 [ν(BH)], 2109 [ν(CO)], 1476, 1356, 1265, 1173, 1138, 1068, 998, 786, 646 cm^{-1}. Anal. Calcd for $C_{16}H_{13}N_6CuOBF_9$: C, 34.90; H, 2.38; N, 15.26. Found: C, 35.36; H, 2.51; N, 15.16.

$Tp^{Ms,H}CuCO$. $Tp^{Ms,H}Cu(THF)$ (0.090 g, 0.127 mmol) was dissolved in a mixture of toluene (1 mL) and pentane (1 mL) in a Schlenk flask, and the solution was then exposed to a CO atmosphere, causing the precipitation of a white powder. Excess CO was removed, the mixture was filtered, and the product was washed with a small amount of pentane (0.059 g, 70%): ^1H NMR (300 MHz, benzene-d_6) δ 1.97 (s, 9 H), 2.04 (s, 18 H), 5.92 (d, J = 2.1 Hz, 3 H), 6.65 (s, 6 H), 7.56 (d, J = 2.1 Hz, 3 H) ppm;$^{13}C\{^1H\}$ NMR (75 MHz, benzene-d_6) δ 20.7, 21.1, 105.1, 128.3, 131.4, 134.9, 137.5, 137.6, 151.4 ppm (CO carbon not observed); FTIR (KBr) 2953, 2920, 2462 [ν(BH)], 2079 [ν(CO)], 1482, 1368, 1352, 1183, 1167, 1046, 777, 745 cm^{-1}. Anal. Calcd for $C_{37}H_{40}N_6BCuO$: C, 67.42; H, 6.12; N, 12.75. Found: C, 67.31; H, 6.21; N, 12.77.

$Tp^{CF_3,CH_3}Cu(NO)$. Yellow solutions containing $Tp^{CF_3,CH_3}Cu(NO)$ were prepared either by vacuum-transferring NO(g) into a Schlenk flask with a known concentration of $Tp^{CF_3,CH_3}Cu(CH_3CN)$ dissolved in the appropriate dry, degassed solvent or by injecting a solution of $Tp^{CF_3,CH_3}Cu(CH_3CN)$ via a gastight syringe into a flask that was thoroughly purged with NO(g). These yellow solutions were used immediately or stored at T < 253 K for less than 1 d. Solutions containing Tp^{CF_3,CH_3}-

(28) Perrin, D. D.; Armarego, W. L. F. *Purification of Laboratory Chemicals*, 3rd ed.; Pergamon: New York, 1988.

(29) Kubas, G. J. *Inorg. Synth.* **1979**, *19*, 90−92; **1990**, *28*, 68−70.

(30) Mahapatra, S.; Halfen, J. A.; Wilkinson, E. C.; Pan, G.; Wang, X.; Young, V. G., Jr.; Cramer, C. J.; Que, L., Jr.; Tolman, W. B. *J. Am. Chem. Soc.* **1996**, *118*, 11555−11574.

(31) (a) Trofimenko, S. *J. Am. Chem. Soc.* **1967**, *89*, 3165−3170. (b) Renn, O.; Venanzi, L. M.; Marteletti, A.; Gramlich, V. *Helv. Chim. Acta* **1995**, *78*, 993−1000.

(32) (a) Nishiwaki, T. *J. Chem. Soc. B* **1967**, 885−888. (b) Atwood, J. L.; Dixon, K. R.; Eadie, D. T.; Stobart, S. R.; Zaworotko, M. J. *Inorg. Chem.* **1983**, *22*, 774−779. (c) Elguero, J.; Yranzo, G. I.; Laynez, J.; Jiménez, P.; Menéndez, M.; Catalán, J.; de Paz, J. L. G.; Anvia, F.; Taft, R. W. *J. Org. Chem.* **1991**, *56*, 3942−3947.

Cu(NO) rapidly decomposed to $Tp^{CF_3,CH_3}Cu(NO_2)$ and N_2O when exposed to trace amounts of NO_2(g) (formed from O_2 and NO), so purging solutions with NO(g) is not a suitable method for preparing solutions of $Tp^{CF_3,CH_3}Cu(NO)$ because trace amounts of NO_2(g) may be admitted into the flask as the needle is inserted into the septum. ^{1}H NMR (300 MHz, CD_2Cl_2 or THF-d_8, 213 K < T < 297 K): only signals corresponding to $Tp^{CF_3,CH_3}Cu(CH_3CN)$ were observed. FTIR (CH_2Cl_2, cm^{-1}): 1753 [$\nu(^{15}NO)$ = 1722], using a CH_2Cl_2 solution of Tp^{CF_3,CH_3}-$Cu(CH_3CN)$ as the spectroscopic blank. UV−vis (CH_2Cl_2, nm) 300, 436. EPR (1:1 CH_2Cl_2/toluene or 1:1 THF/toluene, 9.44 GHz, 2 K < T < 297 K): silent.

$Tp^{Ms,H}Cu(NO)$. $Tp^{Ms,H}Cu$(THF) (0.078 g, 0.111 mmol) was dissolved in toluene (5 mL) in a Schlenk flask, and the flask was purged with NO(g). The solution immediately turned dark orange, and an orange precipitate formed. The mixture was filtered, and the solid was briefly dried under a stream of N_2, yielding $Tp^{Ms,H}Cu(NO)$ as a powder (0.060 g, 82% crude yield). Crystalline material was obtained in lower yield by reacting a concentrated THF/pentane solution of $Tp^{Ms,H}$-Cu(THF) (0.150 g, 0.211 mmol) with NO, followed by cooling to 193 K (0.054 g, 34% crude yield). Solid $Tp^{Ms,H}Cu(NO)$ was stored and handled in the glovebox. The complex was unstable as a solid and decomposed when dried completely either with N_2 or by exposure to a vacuum, as evidenced by bleaching of its color. As a result, attempts to obtain satisfactory elemental analyses were unsuccessful. The analogue $Tp^{Ms,H}Cu^{15}NO$ was prepared as a solid in a similar fashion, except ^{15}NO was vacuum-transferred into the reaction flask. Solutions containing $Tp^{Ms,H}Cu(NO)$ were prepared by purging NO(g) over known concentrations of $Tp^{Ms,H}Cu$(THF) in the appropriate dry, degassed solvent and were used immediately or stored at T < 253 K for less than 1 d. Clean solutions of $Tp^{Ms,H}Cu(NO)$ could not be prepared by dissolving crystals or powders of the complex due to the instability of the complex in solution in the absence of NO as well as the low solubility of the solid once it was precipitated from solution. Experimental data: ^{1}H NMR (300 MHz, THF-d_8, 238 K) δ 2.56 (s, 18 H), 2.72 (s, 9 H), 6.47 (s, 3 H), 7.12 (s, 6 H), 12.64 (s, 3 H) ppm; FTIR (KBr) 2975, 2948, 2921, 2472 [ν(BH)], 1711 [$\nu(^{15}NO)$ = 1682], 1484, 1352, 1186, 1167, 1068, 1049, 780, 744, 708 cm^{-1}; UV−vis [THF, nm (ϵ, M^{-1} cm^{-1})] 344 (sh, 2800), 472 (1200); EPR (1:1 CH_2Cl_2/toluene, 9.44 GHz, 4.2 K < T < 297 K) silent.

$Tp^{CF_3,CH_3}Cu(NO_2)$. $Tp^{CF_3,CH_3}Cu(CH_3CN)$ (0.088 g, 0.156 mmol) was dissolved under N_2 in dry, degassed CH_2Cl_2 (5 mL). Purified NO (1 atm) was vacuum-transferred into the reaction flask. After 1 week of stirring, the color changed from yellow to green and a precipitate formed. The NO atmosphere was replaced with N_2, the mixture was filtered, and the collected solid was washed with Et_2O to afford the product as a green microcrystalline material (0.055 g, 62%). The crystal used for X-ray crystallography was prepared by allowing a THF solution (∼3.5 mL) containing $Tp^{CF_3,CH_3}Cu(NO)$ [prepared from 0.054 g of $Tp^{CF_3,CH_3}Cu(CH_3CN)$] to decompose for 2 d. The solvent and excess NO(g) were removed under reduced pressure. The green residue was dissolved in boiling THF (∼4 mL), and Et_2O was diffused into this solution at 278 K to give a few green crystals. Experimental data: FTIR (KBr) 3142, 2572 [ν(BH)], 1466, 1356, 1265, 1203, 1172, 1146, 1131, 1114, 1067, 1010, 811, 800, 646 cm^{-1}; UV−vis [THF, nm (ϵ, M^{-1} cm^{-1})] 296 (3000) 768 (90); EPR (1:1 THF/toluene, 9.44 GHz, 77 K) $g_{\|}$ = 2.31, $g_\perp$ = 2.06, $A_{\|}^{Cu}$ = 148 G, $A_\perp^N$ = 14 G. Anal. Calcd for $C_{15}H_{13}N_7CuBF_9O_2$: C, 31.68; H, 2.3; N, 17.24. Found: C, 31.82; H, 2.24; N, 17.08.

$Tp^{Ms,H}Cu(NO_2)$. This complex was isolated in quantitative yield from the reaction of NO with $Tp^{Ms,H}Cu$(THF) (0.100 g, 0.142 mmol) in THF (4 mL) for 18 h, followed by removal of excess NO and solvent under vacuum. In an independent synthesis, a solution of $TlTp^{Ms,H}$ (0.172 g, 0.223 mmol) in THF (10 mL) was stirred with admixed solutions of $CuCl_2$ (0.090 g, 0.669 mmol) in MeOH (1 mL) and $NaNO_2$ (0.092 g, 1.34 mmol) in MeOH (2 mL) for 30 min. Solvent was removed under reduced pressure, the solid was extracted with CH_2Cl_2 (10 mL), and the extract was filtered. Methanol (2−3 mL) was added to the solution, and the volume was reduced slowly under vacuum until a light green solid precipitated. The product was collected by filtration and air-dried (0.125 g, 83%). The $^{15}NO_2$ compound was prepared by the same procedure, using $Na^{15}NO_2$ instead of $NaNO_2$. Experimental data: FTIR (KBr) 2969, 2939, 2855, 2472 [ν(BH)], 1614, 1483, 1288 [$\nu_a(NO_2)$; $\nu_a(^{15}NO_2)$ = 1266], 1350, 1184 [$\nu_s(NO_2)$; $\nu_s(^{15}NO_2)$ = 1156], 1167, 1049, 880 [δ_a(ONO); $\delta_a(O^{15}NO)$ = 876], 796, 779, 744, 734 cm^{-1}; UV−vis [THF, nm (ϵ, M^{-1} cm^{-1})] 300 (1500), 390 (sh, 260), 778 (70); EPR (9.47 GHz, CH_2Cl_2/toluene, 77 K) $g_{\|}$ = 2.31, $g_\perp$ = 2.06, $A_{\|}^{Cu}$ = 135 G, $A_{\|}^N$ = 10 G, $A_\perp^N$ = 12 G. Anal. Calcd for $C_{36}H_{40}N_7BO_2Cu$: C, 63.86; H, 5.95; N, 14.48. Found: C, 63.96; H, 6.03; N, 14.46.

Determination of N_2O Yields. In a typical experiment for the Tp^{CF_3,CH_3} system, NO(g) (1 atm, 49 mL) was vacuum-transferred into a solution of $Tp^{CF_3,CH_3}Cu(CH_3CN)$ (24 mg, 0.043 mmol) in dry, degassed CH_2Cl_2 (3.0 mL) in a 25 mL Schlenk flask with a glass joint and glass stopper (after ∼1−2 days, septa were degraded by NO). After the solution was stirred for 3 d, the headspace gas and solvent were vacuum-transferred into a Schlenk flask with a rubber septum. The amount of N_2O produced was determined by injecting 10 μL aliquots of headspace gas above the solvent onto a GC column and then comparing the area of the N_2O peak to that of a standard curve. The standard curve was created by adding CH_2Cl_2 (3.0 mL) to the same Schlenk flask and then vacuum-transferring in NO(g) (49 mL) plus 0, 1, or 2 mL of pure N_2O. Samples of the headspace gas (10 μL volume) were injected onto the GC column, and a plot of the moles of N_2O in the flask versus the area of the N_2O peak was used to generate the standard curve. For the Tp^{CF_3,CH_3} system, the yield of N_2O measured by this method based on moles of copper was 60%. In a typical experiment for $Tp^{Ms,H}$, a solution of $Tp^{Ms,H}Cu$(THF) (30 mg, 0.043 mmol) in THF (3.0 mL) was injected into a 25 mL Schlenk flask which was purged with NO(g) and the solution was stirred for 18 h (a rubber septum could be used due to the shorter exposure time). The amount of N_2O produced was determined by GC in the same manner as described for Tp^{CF_3,CH_3}. For the $Tp^{Ms,H}$ system, the yield of N_2O measured by this method based on moles of copper was 97%.

Kinetics Experiments for the Disproportionation Reactions of $Tp^{R,R'}Cu(NO)$. In a typical experiment, $Tp^{CF_3,CH_3}Cu(CH_3CN)$ (10 mg, 0.012 mmol) dissolved in CH_2Cl_2 (4 mL) was transferred to a 10 mL test tube equipped with a stirbar, a UV cell side arm, and a Teflon stopcock (total volume of the empty UV flask was 45 mL). The solution was then frozen in liquid N_2, and the tube was evacuated. Purified NO gas (81 mL, 1.97 atm) was then transferred into the flask. The solution was quickly warmed to 297(1) K and placed in a constant-temperature bath for ∼5 min to equilibrate prior to beginning data acquisition. Solutions of $Tp^{Ms,H}Cu(NO)$ in THF were prepared in a similar fashion. The electronic spectra were measured every 900 or 300 s for Tp^{CF_3,CH_3} or $Tp^{Ms,H}$, respectively, with vigorous stirring of the solution in the bath between each data point collection. For the Tp^{CF_3,CH_3} system, the data collection was ended after about 5−6 h (∼1−3 half-lives) because the final product precipitated out of solution. The infinity readings for Tp^{CF_3,CH_3} were determined using the Kezdy−Swinbourne treatment.[33] For the $Tp^{Ms,H}$ system, data were collected for 4−5 half-lives, and an infinity spectrum was collected after 8−10 half-lives. Slight adjustments (<5%) of the infinity spectrum gave improved first-order fits. To correct for slight variations in the baseline, the data sets were adjusted by setting the isosbestic point to zero absorbance for all scans. The changes in absorbance at 436 and 768 nm for Tp^{CF_3,CH_3} or 472 and 778 nm for $Tp^{Ms,H}$ versus time were fit to first-order plots. Kinetics experiments to determine the [NO] dependence of the reaction were conducted using a 4.78 mM stock solution of $Tp^{Ms,H}Cu$(THF) in THF. These experiments were performed as mentioned above, except the NO concentration in solution was varied by vacuum-transferring in different amounts of NO to obtain final pressures of 0.67, 0.97, 1.50, and 1.97 atm.

X-ray Crystallography. Crystals of $Tp^{CF_3,CH_3}Cu(CH_3CN)$, $Tp^{Ms,H}$-Cu(THF), and $Tp^{CF_3,CH_3}Cu(NO_2)$ were attached to glass fibers and mounted on an Enraf-Nonius CAD4 [Cu(I) complexes] or Siemens SMART system [Cu(II)−nitrite complex] for data collection. For the structures determined using the CAD4 instrument, cell constants were determined from a set of 25 reflections determined from a random search routine. For the structure determined using the SMART system,

(33) Espensen, J. H. *Chemical Kinetics and Reaction Mechanisms*; McGraw-Hill: New York, 1981, pp. 24−30.

an initial set of cell constants was calculated from reflections harvested from three sets of 20 frames oriented such that orthogonal wedges of reciprocal space were surveyed; orientation matrices were determined from 85 reflections. Final cell constants were calculated from a set of 4008 strong reflections from the actual data collection. Space groups for all the structures were determined on the basis of systematic absences and intensity statistics, and successful direct-methods solutions were calculated which provided most non-hydrogen atoms. The remaining non-hydrogen atoms were located by several least-squares/difference Fourier cycles. All non-hydrogen atoms were refined with anisotropic displacement parameters unless stated otherwise. All hydrogen atoms were placed in ideal positions and refined as riding atoms with relative isotropic displacement parameters. All calculations were performed with an SGI INDY R4400-SC or a Pentium computer using the SHELXTL V5.0 suite of programs.[34] Crystallographic data are listed in Table 1, selected bond lengths and angles are provided in Table 2, and full descriptions of each structure are provided as Supporting Information.

For $Tp^{CF_3,CH_3}Cu(CH_3CN)$, each of the disordered CF_3 groups was refined as two parts. The C(17) group was refined with each part half occupied. The C(27) and C(37) CF_3 groups refined as 0.64/0.36 and 0.40/0.60% occupied, respectively; SAME and DELU restraints were used on the CF_3 groups in order to maintain sensible bond lengths and angles. The EADP and EXYZ constraints were used on carbon atoms C(17), C(27), and C(37) to keep the positional and displacement parameters of each part equivalent.

(34) *SHELXTL-Plus V5.0*; Siemens Industrial Automation, Inc.: Madison, WI.

For $Tp^{Ms,H}Cu(THF)$, the THF molecule was disordered over three positions defined by the 3-fold Cu−B axis. The THF oxygen atom is offset from the 3-fold axis only slightly, causing unreasonable thermal parameters. Therefore, this oxygen atom was refined isotropically and the THF molecule was restrained using SAME.

For $Tp^{CF_3,CH_3}Cu(NO_2)$, the technique of hemisphere collection was used in which a randomly oriented region of reciprocal space was surveyed to the extent of 1.3 hemispheres to a resolution of 0.84 Å. Three major swaths of frames were collected with 0.30° steps in ω.

Acknowledgment. We thank the NIH (Grant GM47365), the NSF (National Young Investigator Award to W.B.T.), and the Alfred P. Sloan and Camille and Henry Dreyfus Foundations (fellowships to W.B.T.) for financial support for this research. We also thank M. Keyes for preliminary work on the X-ray crystal structure of $Tp^{CF_3,CH_3}Cu(CH_3CN)$, C. Buss for help with the X-ray structures, and the reviewers for some excellent suggestions.

Supporting Information Available: Text and tables giving full details and results of the X-ray crystal structure determinations, additional structural diagrams, and the derivation of eqs 3−5 (36 pages, print/PDF). See any current masthead page for ordering information and Web access instructions.

JA982172Q